APPLIED PHYSICS LETTERS **90**, 191501 (2007)

Stability and tunability of the gyrotron backward-wave oscillator

T. H. Chang,[a] C. T. Fan, K. F. Pao, and K. R. Chu
Department of Physics, National Tsing Hua University, Hsinchu 300, Taiwan

S. H. Chen
Department of Physics, National Changhua University of Education, Changhua 500, Taiwan

(Received 6 March 2007; accepted 14 April 2007; published online 7 May 2007)

To fulfill the broadband tunability of the gyrotron backward-wave oscillator (gyro-BWO), stability issues are studied and displayed in the form of stability maps. These maps serve as a guide for the identification and optimization of stable windows for broadband tuning. A Ka-band gyro-BWO experiment was conducted accordingly. In the case of a short interaction length, stable and smooth tunability of 1.3 GHz was demonstrated with a peak interaction efficiency of 29.8%. In the longer length case, piecewise-stable tuning curves were obtained, as predicted in theory. © *2007 American Institute of Physics*. [DOI: 10.1063/1.2737135]

The gyrotron backward-wave oscillator (gyro-BWO) is a promising source of coherent millimeter-wave radiation based on the electron cyclotron maser interaction.[1–4] As illustrated in the ω-k_z diagram of Fig. 1(a), the electron cyclotron frequency is adjusted for synchronous interaction with a backward wave. By employing a nonresonant circuit, the gyro-BWO features continuous frequency tunability by either the beam voltage or magnetic field adjustment. This affords the gyro-BWO a unique capability among all versions of the gyro-devices. However, in most gyro-BWO experiments, ragged[3] or even discrete[2,4] power outputs were observed during the magnetic field and voltage tunings.

The current study primarily aims at the stability issues associated with magnetic field tuning. Probable causes for the erratic frequency tuning include single-mode self-modulation,[5,6] competition from axial modes,[7] and reflections from the external circuit.[8] Our stability analysis will focus on the former two causes, which are intrinsic in nature. On the other hand, an earlier theory[9] predicts that a shorter interaction is an effective remedy for nonstationary oscillations at no expense to the interaction efficiency. A comprehensive stability analysis will be presented in the form of stability maps. On the basis of these maps, both stable and unstable configurations have been tested. The results are found to be in good agreement with theoretical predictions.

Configuration and numerical modeling. A schematic of the Ka-band gyro-BWO optimized for efficiency is shown in Fig. 1(b). The interaction structure (for both theoretical and experimental studies) consists of a uniform middle section of radius r_w=0.267 cm, connected at each end by a 4 cm tapered section to a short uniform section 0.7 cm in length and 0.325 cm in radius. The length (L_0) of the uniform section is chosen to be either 3 or 9 cm. The upstream waveguide taper provides the additional benefit of efficiency enhancement. The slightly up-tapered magnetic field has been experimentally employed principally for the purpose of stabilizing the unwanted oscillations in the coupler section. It also has the effect of slightly increasing the efficiency.[10] However, it bears little significance to the overall stability consideration.

For a systematic investigation of the stability issues, a time-dependent code[7] has been employed in conjunction with a stationary code.[9] The time-dependent code allows the excitation of multiple axial modes. The stationary code yields an equilibrium solution for a single mode regardless of its stability. It complements the time-dependent code by providing useful information on individual mode properties (in particular, the start-oscillation current). The transverse field profiles of the TE_{11} waveguide mode and the outgoing-wave boundary condition are assumed for both codes. The gyro-BWO is relatively insensitive to the velocity spread, so a cold electron beam ($\Delta v_z/v_z$=0) is assumed for the simulations.

The $\alpha(=v_\perp/v_z)$ value of the electron beam depends on the magnetic field (B_0) and the beam voltage (V_b). The simulated α profile in the B_0-V_b space, interpolated between data points, is shown in Fig. 2 and will be used for the simulation of beam-wave interactions over a broad B_0 and V_b tuning range. Table I summarizes the parameters used in the simulation study.

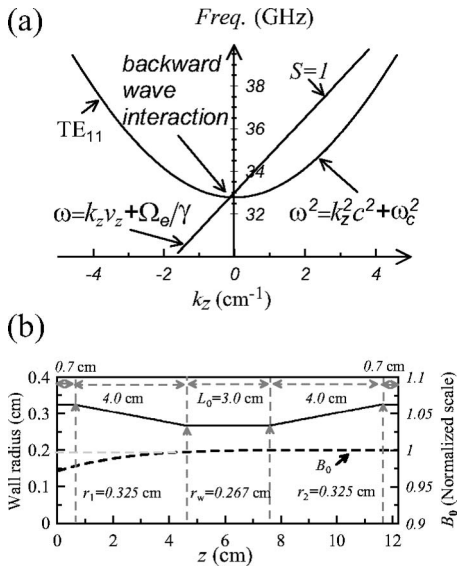

FIG. 1. (a) Operating point of the gyro-BWO in the ω-k_z diagram. Ω_e, v_z, and ω_c are the nonrelativistic cyclotron frequency, the axial velocity of the electrons, and the cutoff frequency of the waveguide, respectively. (b) Profiles of the interaction structure (absolute scale) and the magnetic field (normalized to the uniform field B_0).

[a]Electronic mail: thschang@phys.nthu.edu.tw

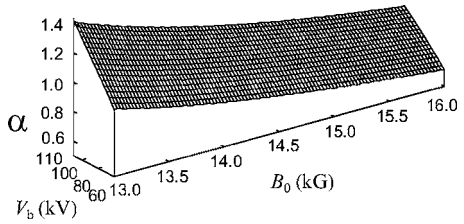

FIG. 2. Simulated α value vs the magnetic field B_0 and beam voltage V_b.

Stability analysis. The time-dependent code is employed to characterize the stability properties with respect to nonstationary oscillations in the I_b-B_0 parameter space. Figures 3(a) and 3(b) display stability maps in the I_b-B_0 space for a fixed beam voltage (V_b=100 kV). Superposed on these maps are the starting currents I_{st} of the first three axial modes obtained with the stationary code. Figure 3 shows excellent agreement between the lowest I_{st} obtained by both codes. However, there is no correlation between the onset current of the nonstationary state and the I_{st} of the next axial mode.

The appearance of multiple zones of nonstationary states has been previously reported[6] in theory. At a fixed beam current, this can lead to nonstationary oscillations in the course of magnetic field tuning. In the interest of avoiding nonstationary oscillations, we focus our attention to identify wide "windows" in the parameter space for maximum range of stable tuning. At our intended operating beam current of 5 A, L_0=3 cm appears to be the optimum choice. The operating beam current is not too far above the lowest I_{st}, which results in greater stability over a broader tuning range. Furthermore, as noted earlier, a shorter interaction length yields the highest efficiency as long as it exceeds approximately half a guide wavelength.

Experimental setup. Figure 4(a) shows a photo of our Ka-band gyro-BWO detached from the superconducting magnet. The electron beam is generated by the magnetron injection gun (MIG) on the left. The electron pitch angle α can be slightly varied through a set of trim coils located at the MIG. Figure 4(b) shows a close-up view of the gyro-BWO circuit mounted to the right of the MIG following a drift section. The output power is measured with a well-calibrated crystal detector (with estimated accuracy of ±5%).

Demonstration of smooth tuning with high efficiency. Figure 3(a) shows that at 5 A, both l=2 and 3 modes could be excited. However, the simulation predicts that the l=2 with its more favorable field profile will be the dominant (hence operating) mode. This has been verified in the experiment described below.

TABLE I. Simulation parameters of the gyro-BWO.

Operating mode	TE_{11}
Cyclotron harmonic	Fundamental
L_0	3 or 9 cm
r_w	0.267 cm
Cutoff frequency (at r_w)	32.92 GHz
Beam current (I_b)	0–20 A
Beam voltage (V_b)	100 kV
Magnetic field (B_0)	13–16 kG
Guiding center position (r_c)	$0.35r_w$
Velocity ratio (α=$v_\perp/v_z$)	See Fig. 2
Velocity spread ($\Delta v_z/v_z$)	0%

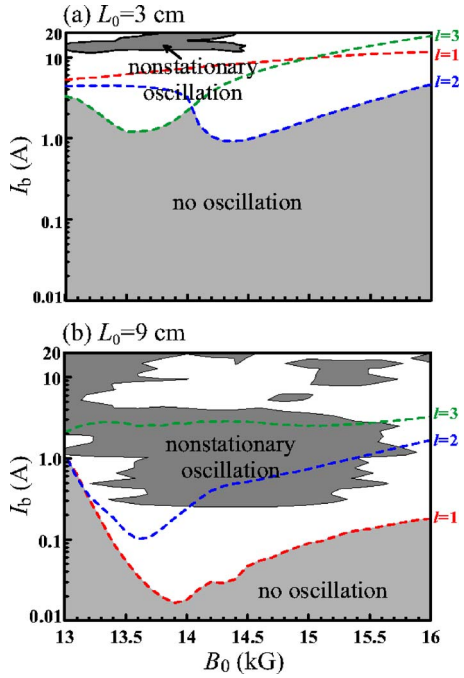

FIG. 3. (Color online) Simulated stability map in the I_b-B_0 space for (a) L_0=3 cm and (b) L_0=9 cm. Other parameters are shown in Table I.

Figure 5 shows the calculated (lines) and measured (dots) efficiencies and frequencies for the magnetic field tuning at I_b=5 A and L_0=3 cm. A smooth 3 dB tuning range of 1.3 GHz was measured with a maximum efficiency of 29.8% at B_0=14 kG, corresponding to a peak output power of 149 kW. The interaction efficiency of 29.8% is the highest achieved to date for the gyro-BWO, but the tuning range (~4%) is moderate compared with recent gyro-BWO experiments.[3] This implies a trade-off between the bandwidth and efficiency which can be exercised in accordance with the specific application need. The calculated and measured data are stationary in the entire tuning range. Apart from the discrepancy at the high magnetic field, low-efficiency end where the velocity spread significantly degrades the efficiency, the measured results are in good agreement with the theory.

Verification of nonstationary tuning with a longer interaction length. We verify the nonstationary tuning which is

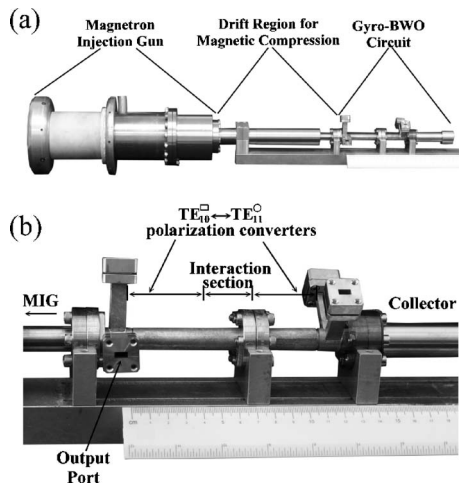

FIG. 4. Photos of the Ka-band gyro-BWO: (a) the whole tube and (b) a close-up view of the interaction circuit.

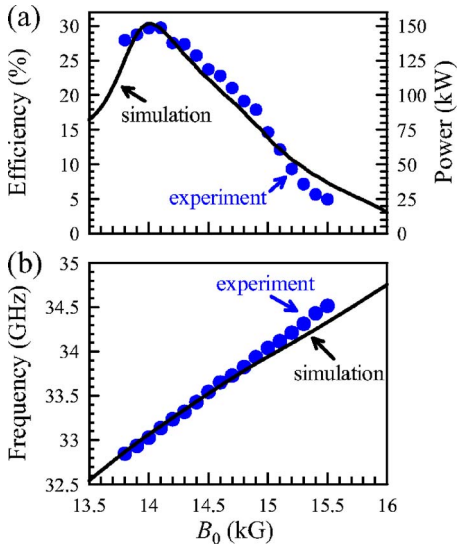

FIG. 5. (Color online) (a) Interaction efficiency and (b) oscillation frequency vs the magnetic field. I_b=5 A, L_0=3 cm, and other parameters are shown in Table I.

more likely to occur for a longer interaction length according to the stability maps of Fig. 3(b). The operating current was lowered to 1.5 A, a value still above the I_{st} of all three axial modes. Nonstationary oscillation, as predicted in Fig. 3(b), has been observed.

Figure 6 shows the calculated (triangles) and measured (circles) results of the magnetic field tuning at I_b=1.5 A and L_0=9 cm. The open triangles and circles denote nonstationary oscillations and the solid triangles and circles denote stationary oscillations. Frequency spectra of the nonstationary oscillations are characterized by a dominant peak and sidebands, which are indicative of single-mode nonstationary behavior.[5] Theory and experiment both show the dominance of the l=1 mode and the same trend in terms of its nonstationary behavior. However, there are regions of disagreement, such as the high B field region due to velocity spread and the stability boundaries. The calculated and measured data are nevertheless in good qualitative agreement.

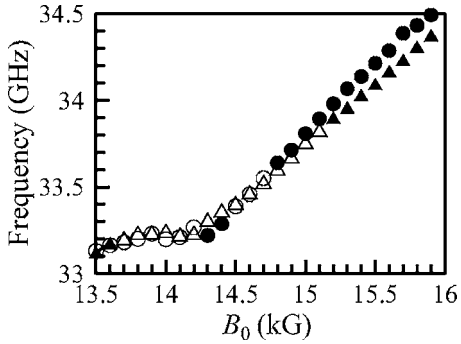

FIG. 6. Simulated and measured oscillation frequency vs the magnetic field. I_b=1.5 A, L_0=9 cm, and other parameters are shown in Table I.

This work was sponsored by the National Science Council, Taiwan. The authors are grateful to the National Center for High-performance Computing for technical supports.

[1]R. H. Pantell, Proc. IRE **47**, 1146 (1959).
[2]M. A. Basten, W. C. Guss, K. E. Kreischer, R. J. Temkin, and M. Caplan, Int. J. Infrared Millim. Waves **16**, 889 (1995).
[3]W. He, A. W. Cross, A. D. R. Phelps, K. Ronald, C. G. Whyte, S. V. Samsonov, V. L. Bratman, and G. G. Denisov, Appl. Phys. Lett. **89**, 091504 (2006).
[4]K. Kamada, K. Nawashiro, F. Tamagawa, H. Igarashi, S. Kizu, C. Y. Lee, S. Kawasaki, R. Ando, and M. Masuzaki, Int. J. Infrared Millim. Waves **19**, 1317 (1998).
[5]T. H. Chang, S. H. Chen, L. R. Barnett, and K. R. Chu, Phys. Rev. Lett. **87**, 064802 (2001).
[6]G. S. Nusinovich, A. N. Vlasov, and T. M. Antonsen, Jr., Phys. Rev. Lett. **87**, 218301 (2001).
[7]K. F. Pao, T. H. Chang, C. T. Fan, S. H. Chen, C. F. Yu, and K. R. Chu, Phys. Rev. Lett. **95**, 185101 (2005).
[8]T. M. Antonsen, Jr., S. Y. Cai, and G. S. Nusinovich, Phys. Fluids B **4**, 4131 (1992).
[9]S. H. Chen, K. R. Chu, and T. H. Chang, Phys. Rev. Lett. **85**, 2633 (2000).
[10]A. K. Ganguly and S. Ahn, Appl. Phys. Lett. **54**, 514 (1989).